

# Supporting Information

Seol et al. 10.1073/pnas.1206480109

## SI Materials and Methods

**Supercoiled (“Coilable”) DNA Preparation.** DNA was constructed with multiple biotin moieties on one extremity and multiple digoxigenin moieties on the other extremity by ligating a 23-kb DNA with two 500-bp DNA handles labeled with either biotin or digoxigenin. The 23-kb DNA was made by PCR using Lambda DNA (New England Biolabs) as a template with primers (1, 2) (forward: 5'-GCGGGTCTCGCAACAATCTGCGATGATGACTATG-3' at 16,944, reverse: 5'-GCGGGTCTCGACCA-GATTTCCACGGATAAGACTC-3' at 40,030; Invitrogen) containing nonpalindromic restriction sites at each end that resulted in ssDNA regions complementary to the DNA handles after digestion. The two “handles” were made by PCR using pBluescript II (Stratagene) as a template and two primers containing non-palindromic restriction sites (forward: 5'-GGACCTGCTTTCGT-TGTGGCGTAATCATGGTCATAG-3', reverse: 5'-GGGTCT-CGTGGTTTATAGTCTGTCGGGTTTC-3'; Invitrogen). For multiple labeling with either biotin or digoxigenin, a small percentage of appropriately labeled dUTP was added to the PCR. PCR products were purified using a Qiagen PCR purification kit and cut with the appropriate restriction endonucleases: BsaI for the digoxigenin-labeled DNA handle, BfuAI for the biotin-labeled DNA handle, and both enzymes for the 23-kb DNA fragment. The biotin- and digoxigenin-labeled DNA handles were ligated to the main DNA segment at room temperature for 3 h.

**Derivation of Religation Probability for the Type IB Topoisomerase Kinetic Scheme.** The “kinetic clutch” model described in Fig. 6 results in the kinetic scheme depicted above. To obtain Eq. 1 in the main text, we proceed as follows.

The religation probability per rotation is derived by summing the probability of religation over all possible pathways from a religation-competent state ( $T \cdot D^c$ ) to a binary complex ( $T \cdot D$ ). The simplest scenario for going into  $T \cdot D$  is  $T \cdot D^c \rightarrow T \cdot D$ , and the probability for this pathway is  $k_L/(k_L + k_f)$ . The second simplest case for ligation is  $T \cdot D^c \rightarrow T \cdot D^{c*} \rightarrow T \cdot D^c \rightarrow T \cdot D$ , where  $T \cdot D^{c*}$  is a rotation-competent state, and the probability for this is the product of the individual probabilities. First, the probability for  $T \cdot D^c \rightarrow T \cdot D^{c*}$  is  $k_f/(k_L + k_f)$ , and for  $T \cdot D^{c*} \rightarrow T \cdot D^c$ , it is  $k_R/(k_R + k_e)$ . Thus, the ligation probability is  $k_f/(k_L + k_f) * k_R/(k_R + k_e) * k_L/(k_L + k_f)$ . The generalized scheme is then

$$\begin{aligned} & \text{Probability of } (T \cdot D^c \rightarrow T \cdot D) \\ & + \\ & \text{Probability of } (T \cdot D^c \rightarrow T \cdot D^{c*} \rightarrow T \cdot D^c \rightarrow T \cdot D) \\ & + \\ & \text{Probability of } (T \cdot D^c \rightarrow T \cdot D^{c*} \rightarrow T \cdot D^c \rightarrow T \cdot D^c \rightarrow T \cdot D^{c*} \rightarrow T \cdot D^c \rightarrow T \cdot D) \\ & + \\ & \vdots \\ & + \\ & \text{Probability of } (T \cdot D^c \rightarrow T \cdot D^{c*} \rightarrow T \cdot D^c)^n \rightarrow T \cdot D \end{aligned}$$

and  $P_{T \cdot D}$  is then

$$\begin{aligned} P_{T \cdot D} &= \frac{k_L}{k_L + k_f} \sum_{n=0}^{\infty} \left[ \frac{k_f}{k_L + k_f} \frac{k_R}{k_R + k_e} \right]^n \\ &= \frac{k_L}{k_L + k_f} * \frac{1}{1 - \frac{k_f}{k_L + k_f} * \frac{k_R}{k_R + k_e}} = \frac{k_L * (k_R + k_e)}{(k_L k_R + k_L k_e + k_f k_e)} \end{aligned}$$

To compute the average uncoiling step size  $\langle n \rangle$  (i.e., the number of turns,  $n$ , relaxed before relegation), we sum over all possible uncoiling step sizes,  $n$ , weighted by the probability of ligation on the  $n$ th rotation:

$$\langle n \rangle = \sum_{n=1}^{\infty} n(1 - P_{T \cdot D})^{n-1} P_{T \cdot D} = 1/P_{T \cdot D}$$

**Pause Time,  $T_c$ , Calculated with a Recursive Relation for the Pause Time Distribution.** Short pauses in rotation, too brief to be considered as type IB topoisomerase (Top1B) unbinding and rebinding events (Fig. 1B), correspond to ligation and cleavage of DNA by Top1B. To obtain the cleavage rate,  $k_c$ , from the measured pause times, we have to account for the contribution of the other kinetic steps that lie between cleavage and the onset of rotation in the kinetic scheme (Fig. 6). The observed pause duration is the time to initiate rotation from the ligated state (i.e., the time from  $T \cdot D$  to DNA rotation,  $T \cdot D_R$ ).

We derive the waiting time using a recursive calculation of the step-time distribution, where the time taken to complete a cycle is related to the amount of time for the first step and the sum of all times to take the remaining steps (3). In this method, the final time distribution,  $\pi_i(t)$ , is defined as the probability density describing how the system goes from a state  $i$  to the final state. The Laplace transform of  $\pi_i(t)$ ,  $\tilde{\pi}_i(s)$ , then serves as the moment-generating function:

$$\tilde{\pi}_i(s) = \sum_{j:j \neq i} \frac{k_{ij} \pi_j(s)}{\sum_{m:m \neq i} k_{im} + s}$$

Using this, we can obtain the time distributions for all steps in the kinetic scheme:

$$\begin{aligned} \tilde{\pi}_{T \cdot D}(s) &= \frac{k_c \tilde{\pi}_{T \cdot D^c}(s)}{k_c + s} \\ \tilde{\pi}_{T \cdot D^c}(s) &= \frac{k_L \tilde{\pi}_{T \cdot D}(s) + k_f \tilde{\pi}_{T \cdot D^{c*}}(s)}{k_L + k_f + s} \\ \tilde{\pi}_{T \cdot D^{c*}}(s) &= \frac{k_e \tilde{\pi}_{T \cdot D_R}(s) + k_R \tilde{\pi}_{T \cdot D^c}(s)}{k_e + k_R + s} \end{aligned}$$

$$\tilde{\pi}_{T \cdot D_R}(s) = 1$$

Solving for  $\tilde{\pi}_{T,D}(s)$  gives

$$\tilde{\pi}_{T,D}(s) = \frac{k_c k_f k_e}{(k_c + s) * [(k_L + k_f + s) * (k_c + k_R + s) - k_f k_R] - k_c k_L * (k_c + k_R + s)}$$

and the average waiting time is

$$T_c = - \left. \frac{\delta \tilde{\pi}_{T,D}(s)}{\delta s} \right|_{s=0} = \frac{k_f k_e + k_c k_L + k_R k_L + k_c k_e + k_c k_R + k_f k_c}{k_c k_e k_f}$$

Because  $1/k_f \ll 1/k_L$  and  $k_R/(k_e k_f) \ll 1$  according to the fit parameters (main text), we can simplify further as

$$k_c \approx \frac{k_L/k_f \left( k_R/k_e + 1 \right) + 1}{\left( T_c - \frac{1}{k_e} \right)}$$

**Single-Energy Barrier Model for Torque Dependence of the Supercoil Relaxation Rate.** In the single-energy barrier model, the rate of supercoil relaxation is governed by a single energy barrier associated with rotation of the DNA 5' free end as shown in Fig. S4A

(4). Torque on the DNA tilts the rotation energy landscape, which lowers the energy barrier and increases the rotation rate. For this simple scenario, the relationship between applied torque and relaxation rate depends on the height of the energy barrier and the transition angle (i.e., the angle between the minimum and maximum energies) (Fig. S4A) and can be explicitly calculated:

$$k_e = 2\pi r_0 \exp(-\beta E_b) [\exp(\Gamma\theta\beta)] \quad \text{[S1]}$$

where  $k_e$  is the relaxation rate;  $r_0$  is the rate of thermal fluctuations,  $r_0 \sim (\beta \eta l^3)^{-1}$  [where  $\eta$  is the buffer viscosity ( $\sim 10^{-3}$  Pa·s) and  $l$  is the radius of DNA (1 nm)],  $E_b$  is the energy barrier,  $\Gamma$  is the external torque,  $\theta$  is the transition angle, and  $\beta = 1/k_B T$  is the inverse of the thermal energy (4). The energy barrier and the transition angle were obtained by fitting the uncoiling rate as a function of torque with this equation.

1. Pommier Y, Marchand C (2012) Interfacial inhibitors: Targeting macromolecular complexes. *Nat Rev Drug Discov* 11:25–36.
2. Ioanoviciu A, et al. (2005) Synthesis and mechanism of action studies of a series of norindenoisoquinoline topoisomerase I poisons reveal an inhibitor with a flipped orientation in the ternary DNA-enzyme-inhibitor complex as determined by X-ray crystallographic analysis. *J Med Chem* 48:4803–4814.
3. Nitiss JL (2009) Targeting DNA topoisomerase II in cancer chemotherapy. *Nat Rev Cancer* 9:338–350.
4. Taneja B, Schnurr B, Slesarev A, Marko JF, Mondragón A (2007) Topoisomerase V relaxes supercoiled DNA by a constrained swiveling mechanism. *Proc Natl Acad Sci USA* 104:14670–14675.

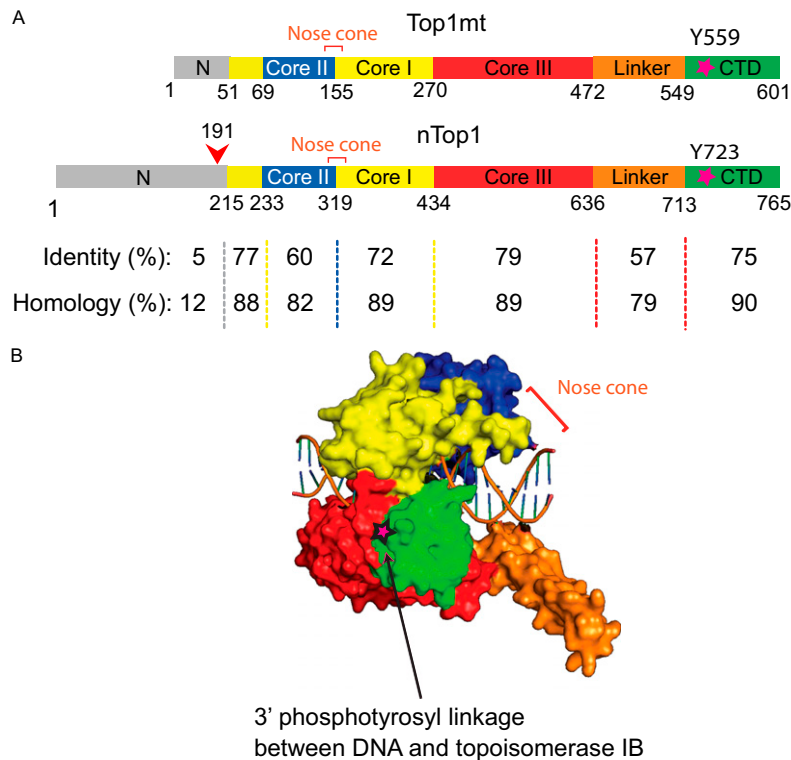


**Fig. S1.** Sequence alignment of human nuclear Top1B (nTop1) and mitochondrial Top1B (Top1mt). (A) Amino acid sequence identity and similarity between nTop1 and Top1mt (1, 2). Note that the core I domain (yellow) is intersected by the core II domain (blue). The red mark at residue 191 indicates the first amino acid position of the N-terminal deletion mutant of nTop1 (Top68). (B) Domains in the space-filling representation of the nTop1 structure [Protein Data Bank (PDB) ID code 1A36] are colored according to the sequence alignment shown in A. The DNA-bound catalytic tyrosine is designated with a star (magenta).

1. Pommier Y (2009) DNA topoisomerase I inhibitors: Chemistry, biology, and interfacial inhibition. *Chem Rev* 109:2894–2902.
2. Zhang H, Meng L-H, Pommier Y (2007) Mitochondrial topoisomerases and alternative splicing of the human TOP1mt gene. *Biochimie* 89:474–481.

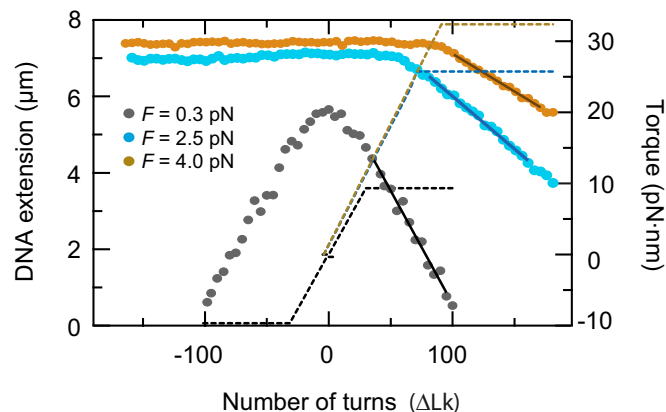


**Fig. S2.** DNA extension (left axis) and torque (right axis) as a function of the number of imposed turns (linking number change,  $\Delta Lk$ ). Extension of 23-kbp DNA was measured as a function of the number of turns; positive and negative directions correspond to the DNA chirality. Torque on the DNA, which is proportional to the DNA twist, was controlled by rotating the tethered bead at different applied tensions ( $F$ ). Following the buckling transition, at which point further rotation of the bead is converted to DNA writhe, the torque on the DNA (DNA twist) remains constant (1). Thus, torque can be controlled by applied tension because the buckling transition occurs at a higher twist density as the tension increases (2). At  $F = 0.3$  pN (black circle), DNA extension decreases symmetrically for both positive and negative turns. At  $F = 2.5$  pN (blue circle) and  $F = 4$  pN (brown circle), DNA extension decreases only for positive turns. The torque applied to the DNA (dashed lines) increases linearly with the number of imposed turns, until the buckling transition and remains constant after the transition. The torque was computed at each force (2) and is represented by dashed lines: black ( $F = 0.3$  pN), blue ( $F = 2.5$  pN), and brown ( $F = 4$  pN). The linearly decreasing regions of the DNA extension vs. rotation curves were fitted with a line to obtain the conversion factor relating extension change to turns (turn/nm) represented with solid lines: black ( $F = 0.3$  pN, 59 nm/turn), blue ( $F = 2.5$  pN, 27 nm/turn), and brown ( $F = 4$  pN, 20 nm/turn).

1. Strick TR, Allemand JF, Bensimon D, Bensimon A, Croquette V (1996) The elasticity of a single supercoiled DNA molecule. *Science* 271:1835–1837.
2. Marko JF (2007) Torque and dynamics of linking number relaxation in stretched supercoiled DNA. *Phys Rev E Stat Nonlin Soft Matter Phys* 76:021926.

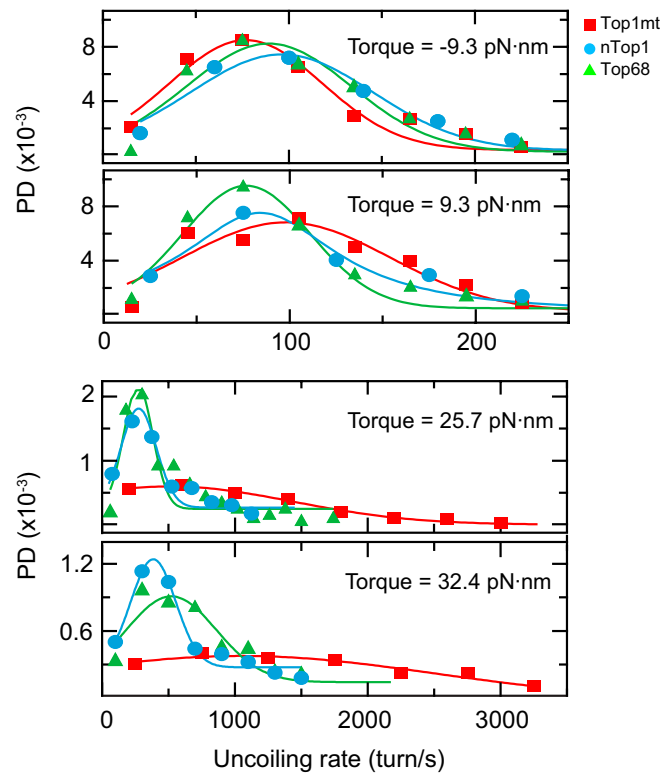


**Fig. S3.** Probability density (PD) of uncoiling rate distributions. Uncoiling rate PD distributions at four different torques on the DNA for mitochondrial Top1B (Top1mt; red squares; number of samples,  $n = 248\text{--}532$ ), nuclear Top1B (nTop1; blue circles;  $n = 257\text{--}481$ ), and N-terminal deletion mutant of nTop1 (Top68; green triangles;  $n = 173\text{--}359$ ). Gaussian fits are represented by solid lines. Uncoiling rates (turns/s) were obtained by dividing linear velocities by a conversion factor at each force (Fig. S2). Negative torque indicates negative turns.

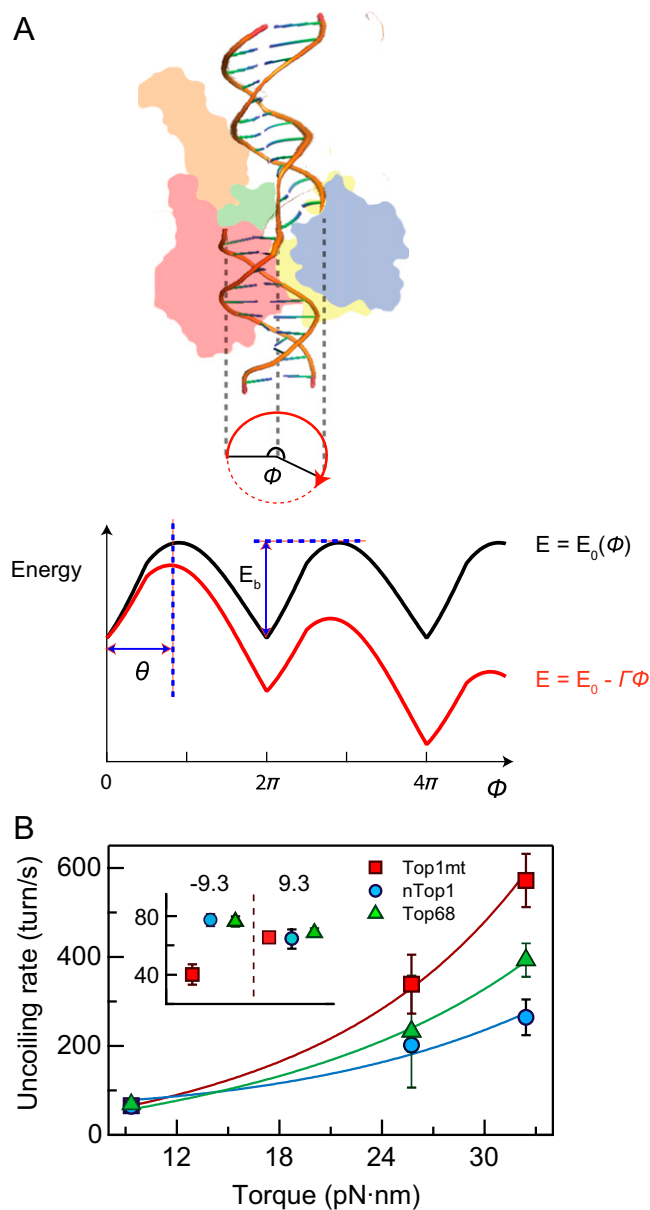


**Fig. 54.** (A) Cartoon of 5' DNA end rotation around intact strand and the energy profile associated with the rotation angle. The rotation of the 5' DNA end is modeled as a random walk over an energy landscape  $[E(\phi)]$  that prevents free rotation of the DNA in the protein clamp. Although the exact profile is not known, the simplest profile (black line) consists of a single energy minimum located near the rotation angle,  $\phi = 0$ , where the DNA cross-section is minimal and an energy barrier ( $E_b$ ) located near  $\phi = \pi$  (dashed line), where the DNA cross-section is maximal (1). Applied torque ( $\Gamma$ ) tilts the energy landscape (red line) and lowers the energy barrier with respect to the energy minimum. (B) Uncoiling rates from Gaussian fits of the velocity distributions (Fig. S3) are plotted as a function of torque and fitted with the barrier-crossing model: mitochondrial Top1B (Top1mt; red square), nuclear Top1B (nTop1; blue circle), and N-terminal deletion mutant of nTop1 (Top68; green triangle). The barrier-crossing fits to Eq. S1 (solid lines). All reported errors are SDs. (Inset) Uncoiling rates of Top1mt, nTop1, and Top68 at positive torque (9.3 pN·nm) and negative torque (-9.3 pN·nm).

1. Wereszczynski J, Andricioaei I (2010) Free energy calculations reveal rotating-ratchet mechanism for DNA supercoil relaxation by topoisomerase IB and its inhibition. *Biophys J* 99: 869-878.

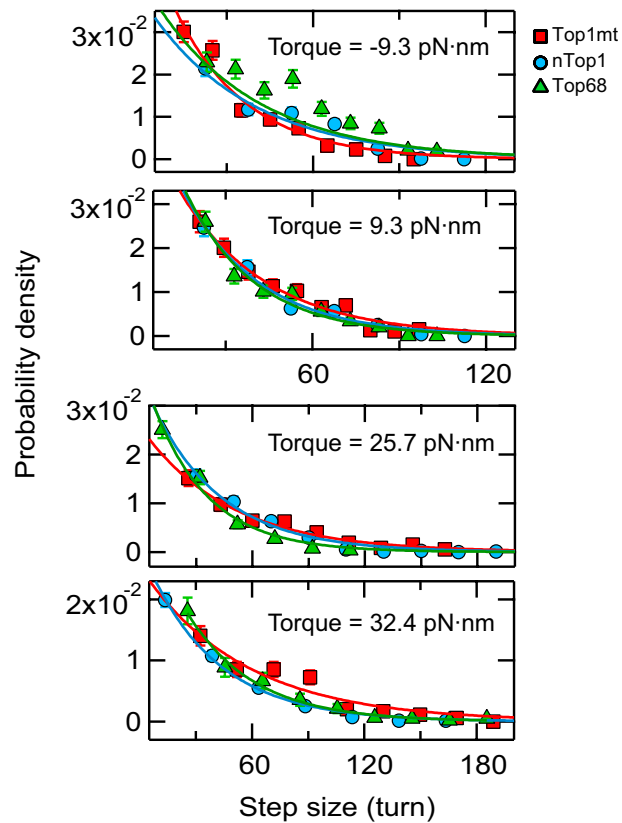


**Fig. S5.** Uncoiling step-size distributions of three Top1B enzymes. Uncoiling step-size probability distributions for Top1B enzymes under different torques were fitted with exponentials to obtain the mean uncoiling step sizes shown in Fig. 3A. The errors correspond to the square root of the number of events in each bin normalized by the total area. Mitochondrial Top1B (Top1mt; red squares; number of events measured at each torque,  $n = 336$ – $552$ ), nuclear Top1B (nTop1; blue circles;  $n = 403$ – $619$ ), and N-terminal deletion mutant of nTop1 (Top68; green triangles;  $n = 309$ – $546$ ).

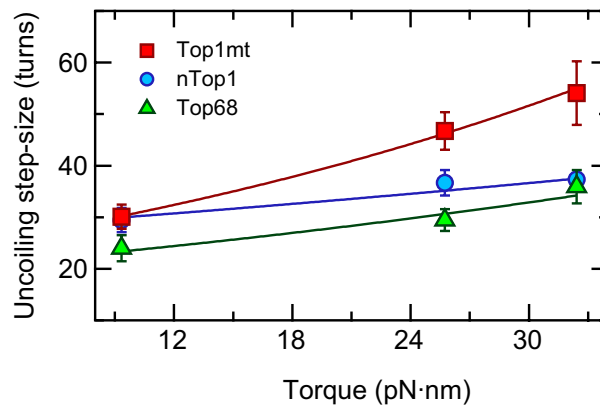


**Fig. 56.** Uncoiling step size as a function of torque fit with the single energy barrier-crossing model. The uncoiling step sizes (turns) for three different enzymes are plotted as a function of torque ( $\Gamma$ ) and fitted with the barrier-crossing model,  $N_0 \exp(\Gamma \theta_t / \beta)$  (solid lines) (1). Here,  $N_0$  and  $\theta_t$  are fitting parameters.  $N_0$  represents the uncoiling step size at zero torque, and  $\theta_t$  is the transition angle corresponding to the angular separation between the energy minimum and the transition state of the barrier. For mitochondrial Top1B (Top1mt),  $N_0$  is estimated to be  $23.7 \pm 2.8$  turns and  $\theta_t$  is  $0.11 \pm 0.02$  radians. For nuclear Top1B (nTop1),  $N_0$  is  $27.4 \pm 2.9$  turns and  $\theta_t$  is  $0.04 \pm 0.01$  radians.  $N_0$  for N-terminal deletion mutant of nTop1 (Top68) is  $20 \pm 3.1$  turns, which is slightly smaller than those of the others two enzymes, and  $\theta_t$  for Top68 is  $0.07 \pm 0.03$  radians, which is larger than that of nTop1 but smaller than that of Top1mt. All reported errors are SDs.

1. Koster DA, Croquette V, Dekker C, Shuman S, Dekker NH (2005) Friction and torque govern the relaxation of DNA supercoils by eukaryotic topoisomerase IB. *Nature* 434:671–674.

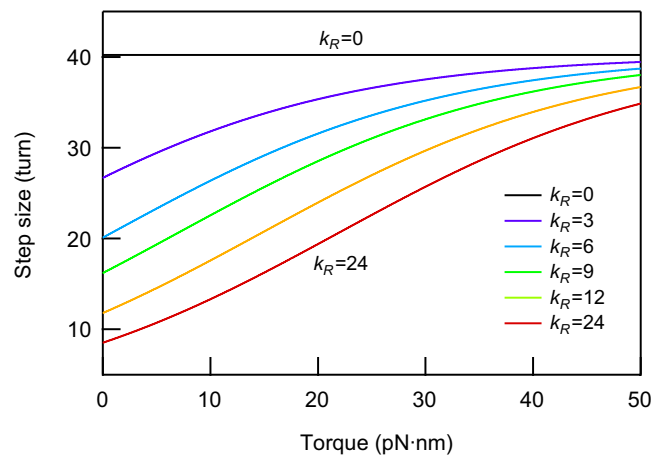


**Fig. 57.** Kinetic tuning of relaxation torque dependence in the "kinetic clutch" model. Relaxation step size as a function of torque for different values of the torque-independent rate  $k_R$  is plotted as function of torque. The step sizes are calculated using Eq. 1 in the main text based on the rates measured for nuclear Top1B (nTop1) but with different values of  $k_R$ . The step size becomes insensitive to torque as  $k_R$  becomes close to zero, indicating how  $k_R$  affects the torque sensitivity of step size or religation probability.

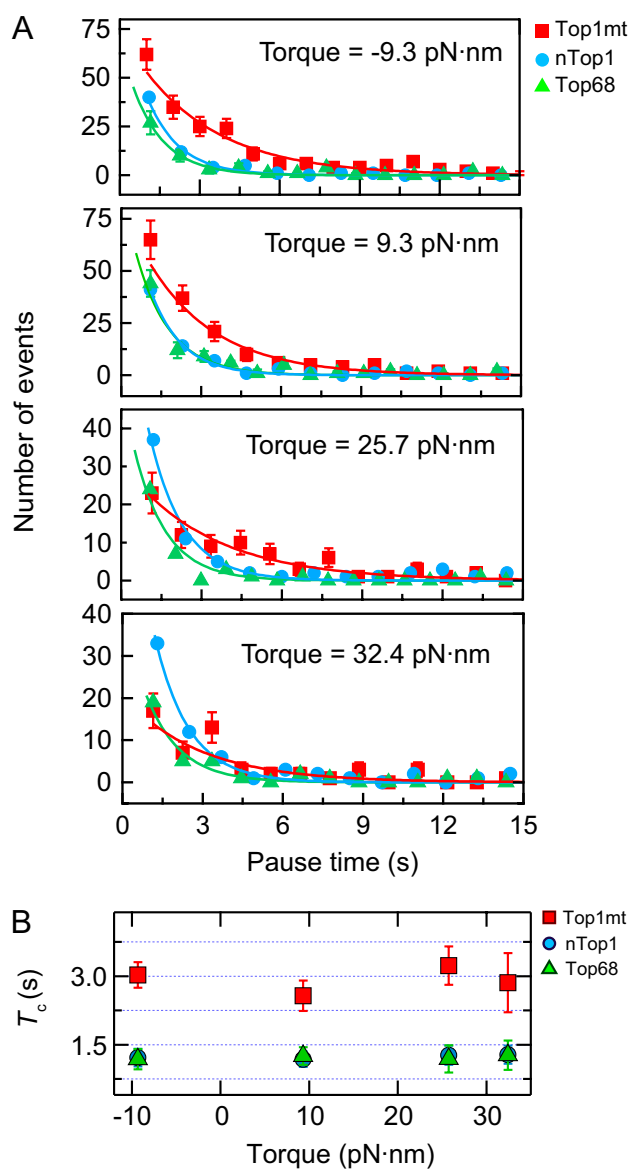


**Fig. S8.** Pause time,  $T_c$ , distributions of three Top1B enzymes. (A) Distributions of  $T_c$  for Top1B enzymes under different torques were fitted with single exponentials to obtain  $T_c$ . The reported errors correspond to the square root of the number of events in each bin. Mitochondrial Top1B (Top1mt; red squares;  $n = 84-239$ ), nuclear Top1B (nTop1; blue circles;  $n = 71-92$ ), and N-terminal deletion mutant of nTop1 (Top68; green triangles;  $n = 76-197$ ). (B)  $T_c$  from single exponential fitting for Top1B enzymes plotted as a function of torque. All reported errors are SDs.



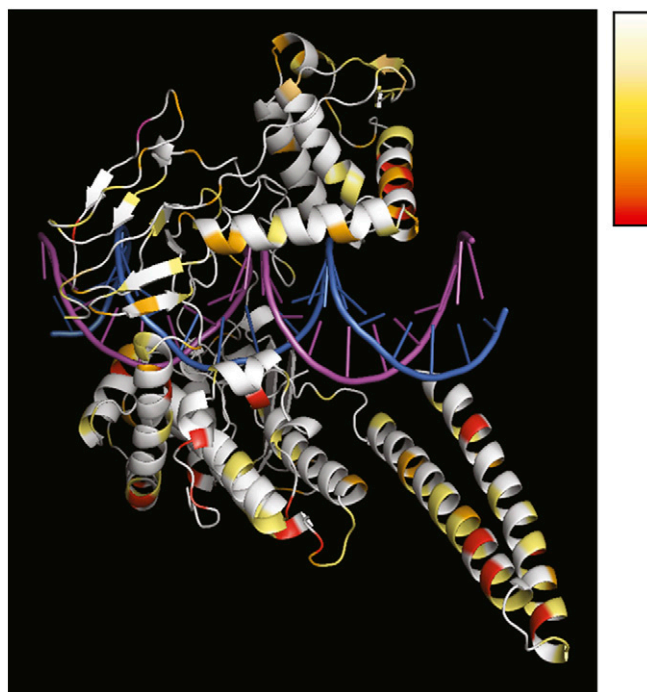


**Fig. S9.** Sequence conservation index map of human Top1B paralogs. Sequence differences between nuclear Top1B (nTop1) and mitochondrial Top1B (Top1mt) were mapped onto the nTop1 structure [Protein Data Bank (PDB) ID code 1A36]. Differences between nTop1 and Top1mt sequence are color-coded based on the conservation index from ClustalW (European Bioinformatics Institute). White indicates sequence conservation, and light yellow to red indicates the degree of sequence similarity (i.e., light yellow indicates high similarity, red indicates low similarity).